Mid-Frequency Signal Fluctuations and Target Localization

W.S. Hodgkiss, G.L. D'Spain, and D.E. Ensberg

Marine Physical Laboratory, Scripps Institution of Oceanography, La Jolla, CA, 92093-0701, USA

Abstract. Environmental fluctuations (e.g. water column sound speed perturbations due to internal waves) result in variability of the vertical arrival angle structure observed from an acoustic source at a given range and depth. Experimental data collected by MPL in 2001 with a mid-frequency, vertical aperture receiving array in shallow (~165 m deep) water provided an opportunity to measure both environmental and the resulting acoustic fluctuations. The variability of both shallow and deep 3.5 kHz source transmissions from 4 km and 2.5 km range is summarized statistically using histograms of signal vertical angle of arrival. These appear to indicate that shallow source arrivals fluctuate more than deep source arrivals. In addition, the use of relatively short-range (~1.0-1.7 km) 3.5 kHz source arrivals (direct path and surface bounce) observed on the vertical array to estimate source range and depth via backwards ray tracing is discussed. Shallow and deep source localization is shown feasible with a slowly drifting source being localized to within ~200 m in range and ~10 m in depth.

INTRODUCTION

Sound speed fluctuations result in variability of the vertical arrival angle structure observed at an array. Here we focus on shallow water experimental observations of 3.5 kHz transmissions from both quasi-stationary source locations as well as source tows and specifically consider transmissions from both shallow and deep source depths. First, we will summarize statistically the observed signal fluctuations from 4 km and 2.5 km source ranges using histograms of signal vertical angle of arrival. Second, we will use relatively short-range, direct path and surface bounce arrivals to estimate source range and depth via backwards ray tracing

EXPERIMENT

The experimental data discussed was collected in July 2001 on a shallow ridge known as Fortymile Bank located 67 km (36 nm) west of San Diego and 41 km (22 nm) southeast of the southern tip of San Clemente Island. The R/P FLIP was moored in 165 m deep water and deployed a 64-element vertical receiving array buoyed up from the seafloor. The array consisted of two nested, 43-element apertures each spaced half-wavelength at 3.75 and 7.5 kHz, respectively. Both stationary source and source tow transmissions were made from locations along the ridge axis. As shown in Fig. 1, the bathymetry along the ridge has slight range-dependency. A set of 40 sound speed profiles derived from CTD casts taken during the experiment also are shown.

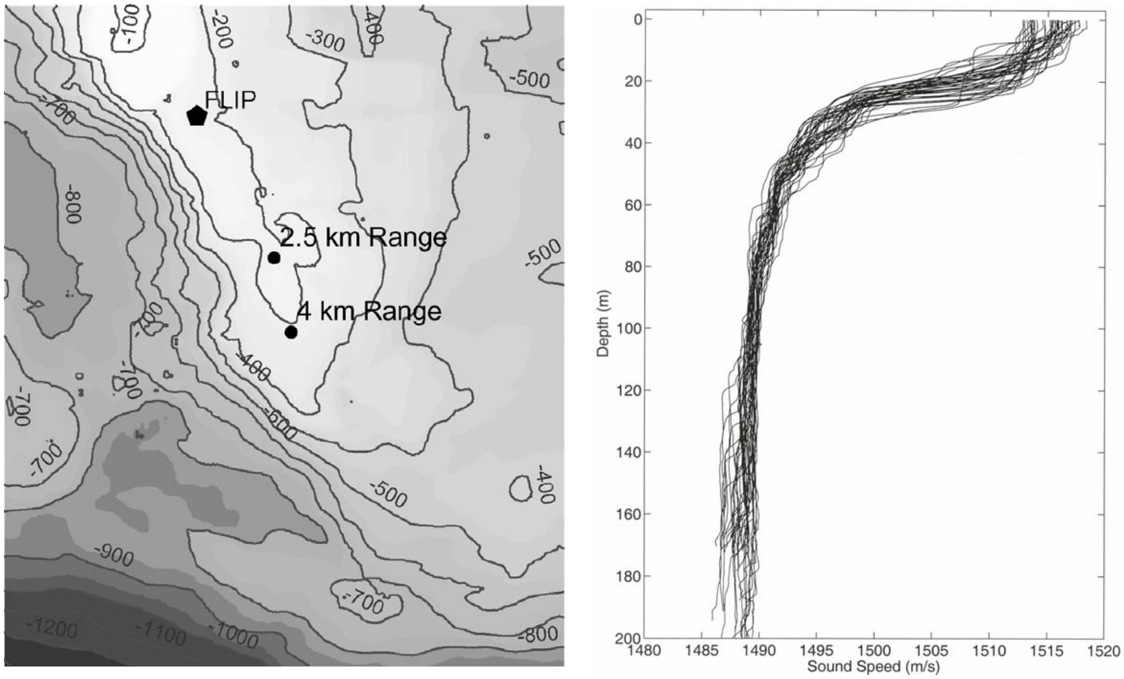

(a) (b)

FIGURE 1. Bathymetry in the vicinity of Fortymile Bank west of San Diego showing the locations of the receiving array deployed from the R/P FLIP and the 2.5 km and 4 km quasi-stationary source stations. Also shown are sound speed profiles derived from 40 CTD casts over the period JD 201-204.

SIGNAL FLUCTUATIONS

Quasi-stationary source transmissions were made from locations 4 km and 2.5 km in range from FLIP. These transmissions were made from several source depths and each was of duration 5 min. Of interest here is a comparison between the arrival structure from shallow (10 m) and deep (70 m) source transmissions.

The observed vertical arrival angle versus time from the 4 km source range is shown in Fig. 2 for these two cases (negative angles correspond to upward looking beams). The presence of near-horizontal arriving energy from the shallow source is due to the range-dependent bathymetry (i.e. slope conversion effects). The largest-level arrivals are in the vicinity of –6.5˚ and –2.5˚ for the 10 m and 70 m source depths, respectively. Histograms of these largest-level arrivals are shown in Fig. 3.

Similarly, the observed vertical arrival angle versus time from the 2.5 km source range is shown in Fig. 4 for the shallow and deep source transmissions. The largest-level arrivals are in the vicinity of –13.5˚ and –4.5˚ for the 10 m and 70 m source depths, respectively. Histograms of these largest-level arrivals are shown in Fig. 5. Note that a second significant arrival dominates the last half of the deep source observations yielding a bimodal distribution of arrival angles.

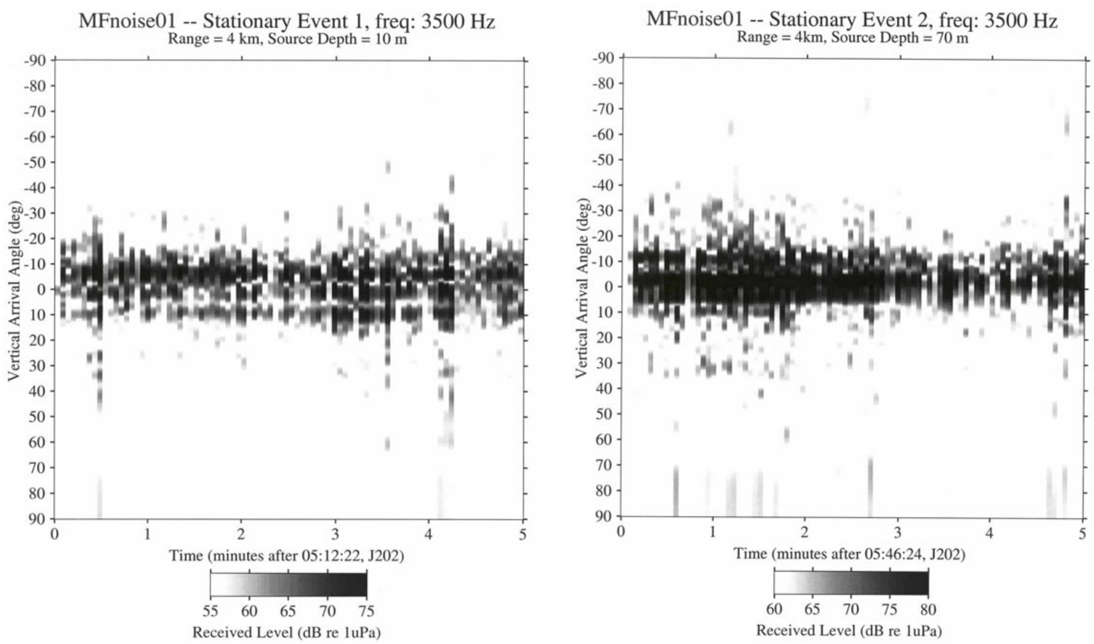

(a) (b)

FIGURE 2. Time-evolving vertical arrival structure for the 10 m (a) and 70 m (b) source depths at the 4 km range source station.

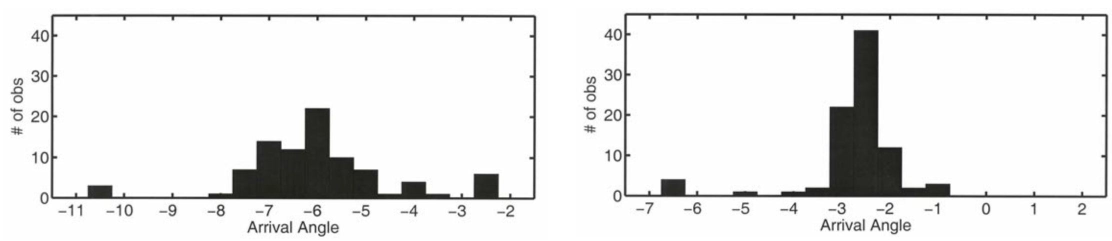

(a) (b)

FIGURE 3. Histograms of vertical arrival structure for the 10 m (a) and 70 m (b) source depths at the 4 km range source station in the vicinity of –6.5˚ and –2.5˚, respectively.

The histograms appear to indicate that the largest level shallow source arrivals fluctuate more than the corresponding deep source arrivals. Analysis of other source depth transmissions (not shown) indicate similar results (e.g. 15 m and 90 m source depths at 4 km range and 16 m and 89 m source depths at 2.5 km range).

TARGET LOCALIZATION

Using a backwards ray tracing approach, the observed arrival angles from shallow and deep source transmissions at relatively close range were used to localize the source in range and depth. Direct path and surface bounce ray arrivals were identified in the receptions and traced backwards to their crossing points using a measured sound speed profile.

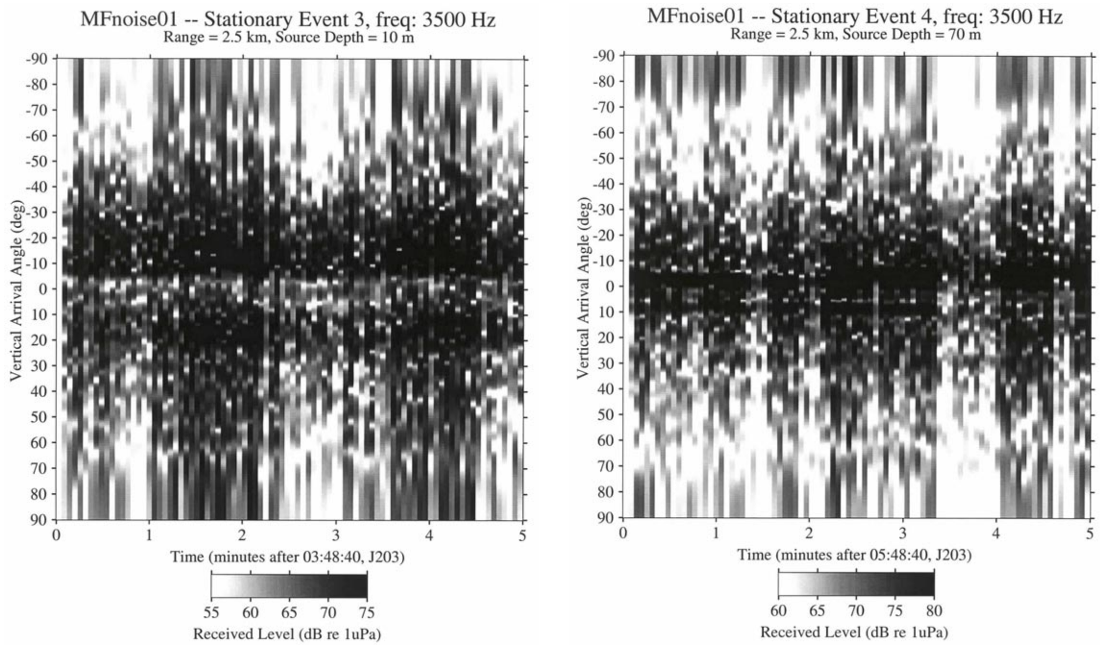

(a) (b)

FIGURE 4. Time-evolving vertical arrival structure for the 10 m (a) and 70 m (b) source depths at the 2.5 km range source station.

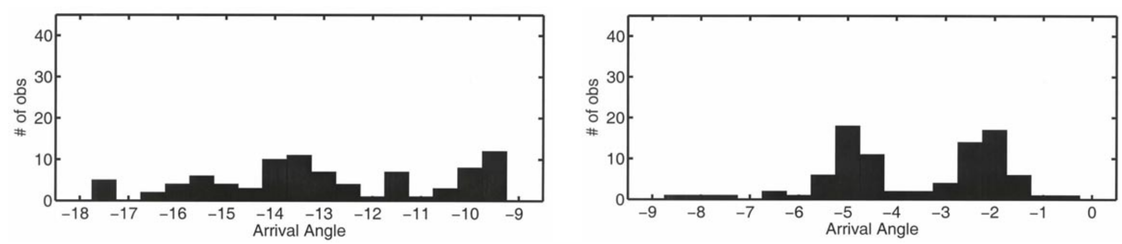

(a) (b)

FIGURE 5. Histograms of vertical arrival structure for the 10 m (a) and 70 m (b) source depths at the 2.5 km range source station in the vicinity of –13.5˚ and –4.5˚, respectively.

In the first case, the source was drifting slowly at a range of approximately 1.1-1.3 km. The observed vertical arrival angle versus time for shallow (30 m) and deep (70 m) source transmissions is shown in Fig. 6. Examples of carrying out backwards ray tracing from identified arrivals are shown in Fig. 7. Scatter plots of the results are shown in Fig. 8 with the 30 m source transmissions being carried out near a range of 1.04 km and the 70 m source transmissions being carried out near a range of 1.27 km. Although there is some scatter in the results, shallow (30 m) and deep (70 m) source localization is feasible and the sources were localized to within ~200 m in range and ~10 m in depth of their true locations.

In order to investigate the influence of sound speed fluctuations on the results, a simulation was carried out. Representative direct path and surface bounce arrival angles were fixed (-7.5° and –12.5° for the 30 m source and –4.6° and –12.6° for the 70 m source) and traced backwards through the time-evolving sound speed structure based on thermistor string measurements made at FLIP. The resulting scatter plots of

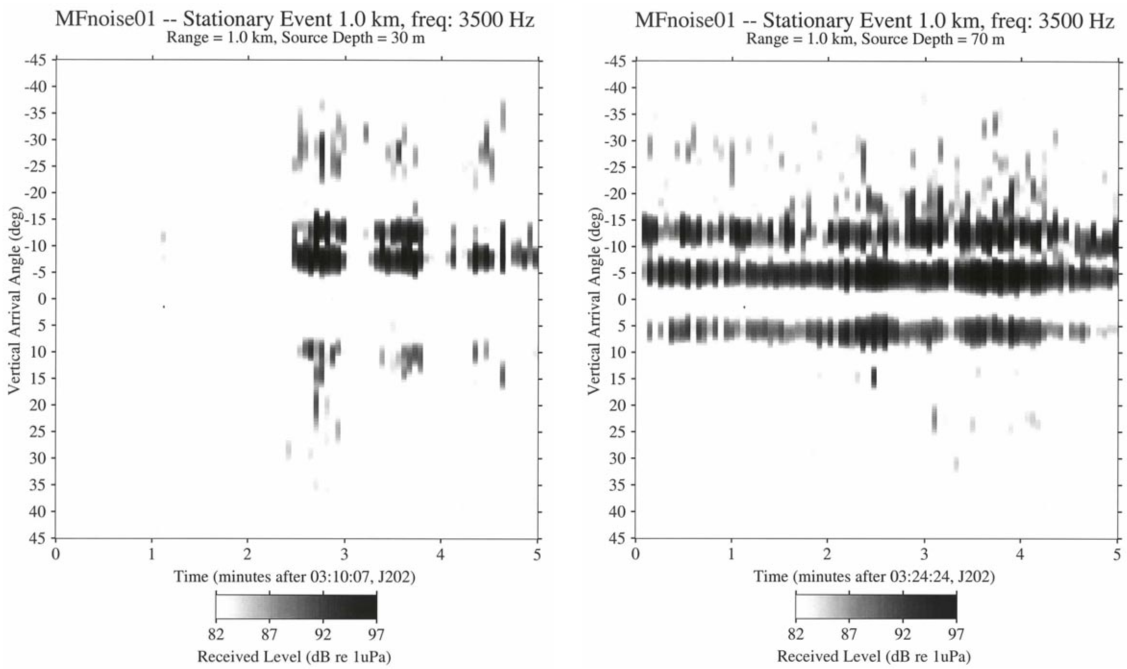

(a) (b)

FIGURE 6. Time-evolving vertical arrival structure for the 30 m (a) and 70 m (b) source depths at ranges 1.04 km and 1.27 km, respectively.

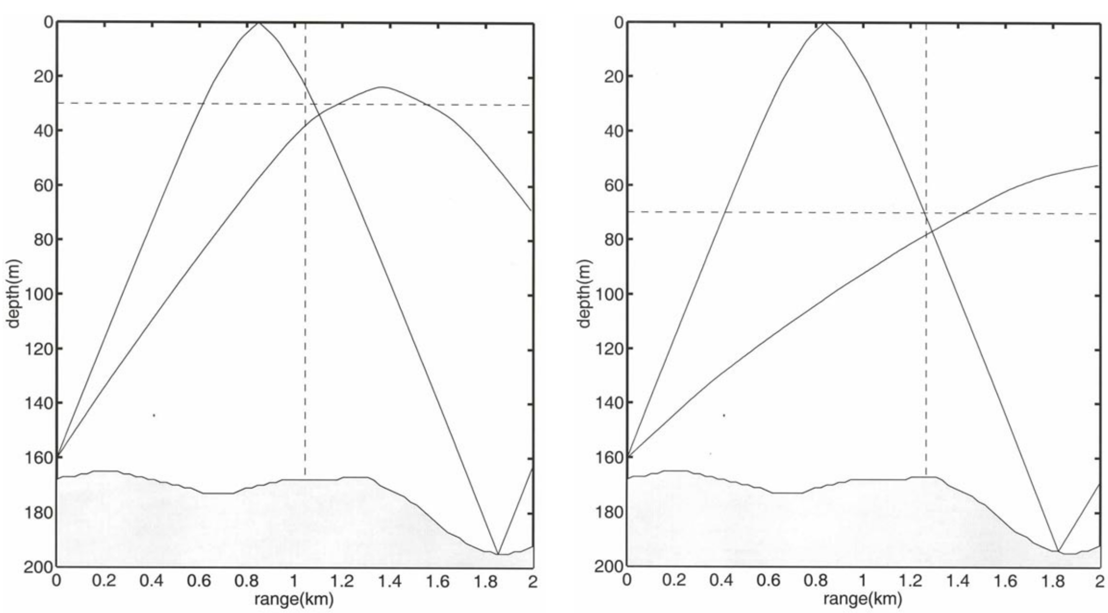

(a) (b)

FIGURE 7. Backwards ray tracing of the direct path and surface bounce arrivals observed from the shallow (30 m) and deep (70 m) source transmissions. The dotted lines indicate the known source locations.

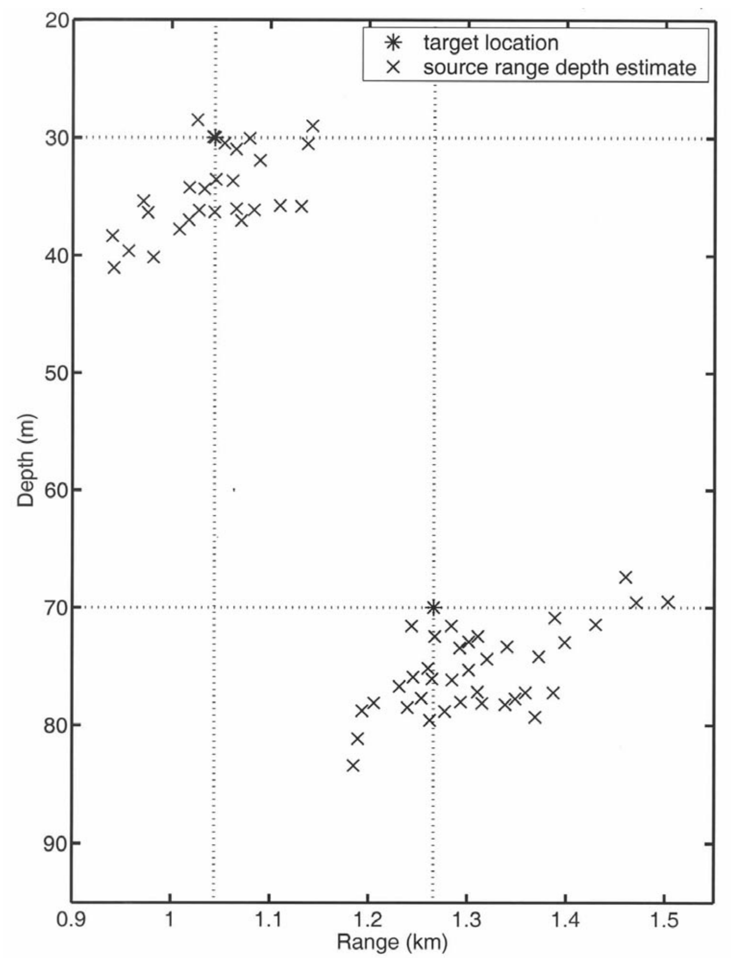

Source Range = 1.04 km

Source Depth = 30 m

Source Range = 1.27 km

Source Depth = 70 m

FIGURE 8. Scatter plots showing the clustering of source range/depth estimates based on backwards ray tracing of the observed arrival angles from the shallow (30 m) and deep (70 m) source transmissions.

the estimates of source range and depth are shown in Fig. 9 which includes both sound speed variation over the 5 min observation periods as well as a larger 7 hour period encompassing the source transmissions. The thermistor string observations over the 7 hour period also are included. The larger scatter in Fig. 8 is a result of the effects of several additional sources of variability not simulated: (1) sea surface roughness, (2) source motion, and (3) error in arrival angle estimation.

In the second set of data analyzed, the source was being towed with the range interval of analysis corresponding to approximately 1.1-1.7 km. The observed vertical arrival angle versus time for shallow (17.5 m) and deep (70 m) sources is shown in Fig. 10. Scatter plots of the results from backwards ray tracing are shown in Fig. 11 with the 17.5 m source transmissions being carried out over a range of 1.08-1.66 km and the 70 m source transmissions being carried out over a range of 1.21-1.69 km. As with the quasi-stationary source transmissions, there is scatter in the results but there is a clear distinction between clusters of shallow and deep source depth estimates.

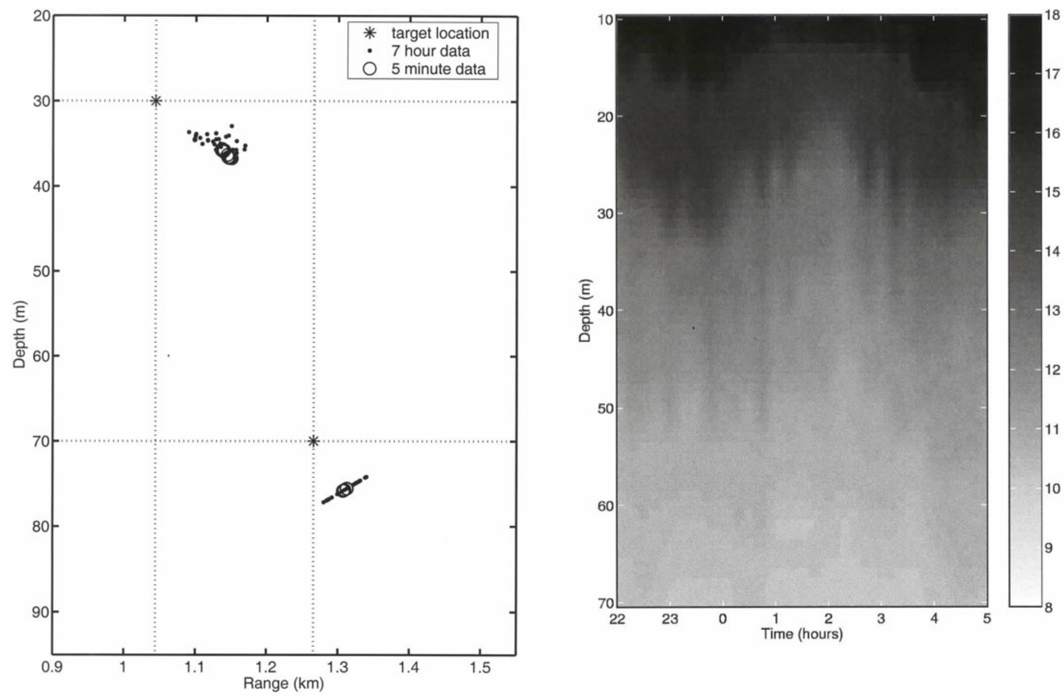

(a) (b)

FIGURE 9. Simulations of range/depth scatter based on observed sound speed fluctuations for fixed arrival angles (a). Both sound speed variability over the 5 min observation periods as well as a larger 7 hour period encompassing the source transmissions is investigated. Thermistor string observations over the 7 hour period also are shown (b).

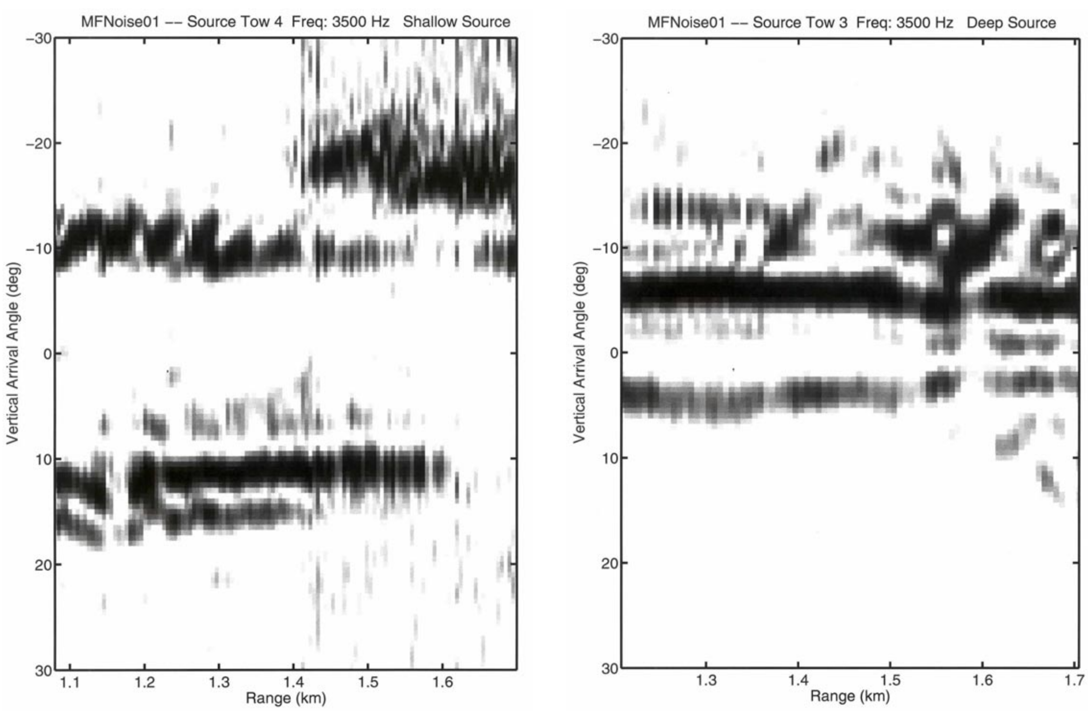

(a) (b)

FIGURE 10. Time-evolving vertical arrival structure for the 17.5 m (a) and 70 m (b) source tow transmissions.

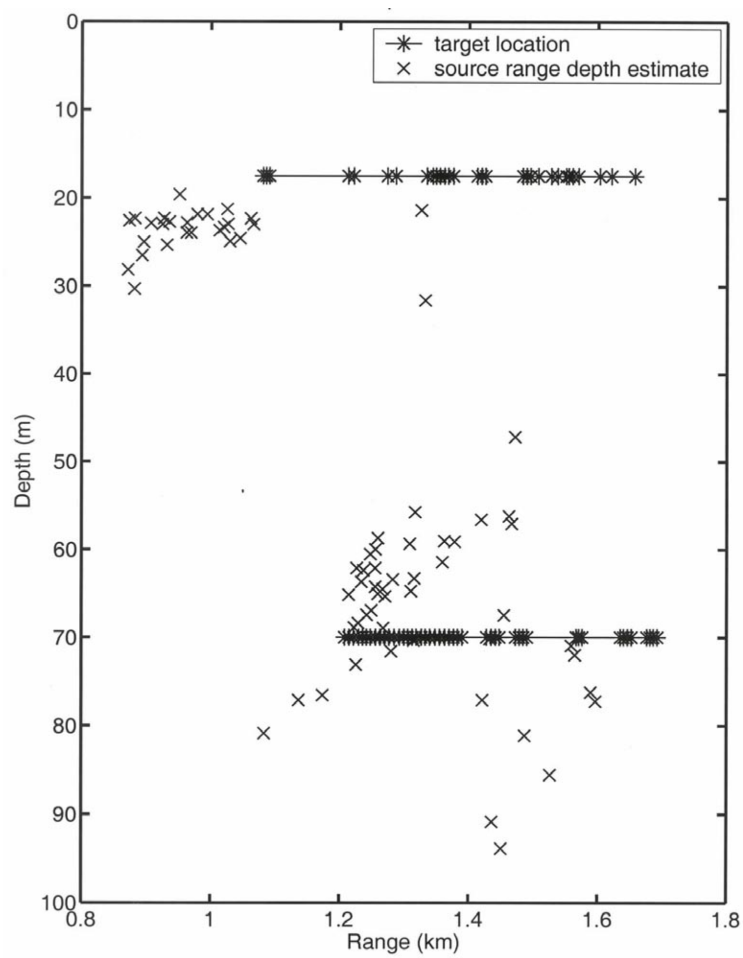

Source Range =
1.08–1.66 km

Source Depth = 17.5 m

Source Range =
1.21-1.69 km

Source Depth = 70 m

FIGURE 11. Scatter plots showing the clustering of source range/depth estimates based on backwards ray tracing of the observed arrival angles from the shallow (17.5 m) and deep (70 m) source tows.

SUMMARY

Experimental data collected with a mid-frequency vertical aperture receiving array in shallow (~165 m deep) water has been analyzed. The variability of both shallow and deep 3.5 kHz source transmissions from 4 km and 2.5 km source ranges has been summarized statistically using histograms of signal vertical angle of arrival. In addition, the use of relatively short range 3.5 kHz source arrivals (direct path and surface bounce) observed on the vertical array to estimate source range and depth via backwards ray tracking has been demonstrated.

ACKNOWLEDGMENTS

This work was supported by the Office of Naval Research, Contract No. N00014-01-D-0043-D01. We also thank Jeff Skinner, Jim Murray, and Katherine Kim who also participated in the experiment.